Copyright 2004 Tech Science Press

Design of Composite Layers with Curvilinear Fiber Paths Using Cellular Automata

Shahriar Setoodeh [1], Zafer Gürdal[2], and Mostafa M. Abdalla [3]

Abstract

Benefits of directional properties of fiber reinforced composites could be fully utilized by proper placement of the fibers in their optimal spatial orientations. This paper investigates an application of a Cellular Automata (CA) based strategy for combined fiber angle and topology design of composite laminae for improved in-plane response. CA are iterative numerical techniques that use local rules to update both field and design variables to satisfy equilibrium and optimality conditions. In the present study, displacement update rules are derived using a local finite element model governing the equilibrium of the cell neighborhood. Local fiber orientation angle and density measure are treated as continuous design variables, and their spatial distribution is determined based on a minimum compliance design formulation. A heuristic pattern matching technique is implemented along with the local optimality condition to maintain fiber orientation continuity in order to improve manufacturability. Numerical examples show the that results are checkerboard free and mesh-independent.

1 Introduction

Manufacturing fiber reinforced laminated composite structures with spatially varying fiber orientation is possible using advanced tow-placement machines. Tow-placement machines are computer numerical controlled multi-axis machines that are capable of steering as many as 36 tows along prescribed paths with some restrictions on the minimum radius of curvature depending on the tow width and type of machine used [1]. Flexibility in steering the fiber tows along curvilinear paths provides new design possibilities that can be

[1]Research Assistant, Engineering Science and Mechanic Department, Virginia Tech

[2]Professor, Departments of Aerospace and Ocean Engineering, and Engineering Science and Mechanics. Currently with the Faculty of Aerospace Engineering at TU Delft.

[3]Research Assistant, Department of Aerospace and Ocean Engineering, Virginia Tech

used to improve mechanical properties of structures made from fiber reinforced laminates. In other words, rather than designing the stacking sequence of laminates with constant ply-angles, each ply can be designed with curvilinear fiber paths that allow variation of the mechanical properties spatially over the structure.

Optimum filament orientation of composites was studied as early as 1970 in an article published by Brandmaier [2], where maximum composite strength was sought by aligning the fiber direction based on local stresses. The article was the first to point out that the optimal fiber orientation could be different from the principal stress direction depending on the strength properties of the lamina. In a series of publications, Pedersen [3, 4, 5, 6, 7] studied optimal fiber orientations by finding local and global extrema of the strain energy density analytically and showed that the optimal fiber orientation depends not only on the ratio of the two principal strains, but also on dimensionless material parameters. Intuitive techniques [8], traditional optimization [9, 10], and optimality criteria [11, 12] are also used in optimum design of laminated composite materials with curvilinear fiber paths. Topology design of isotropic materials is also a very well developed topic in the structural optimization community. Extensive mathematical models have been developed and successfully applied to design structures such as trusses, beams, and plates. In the case of two dimensional plates, Solid Isotropic Material Penalization (SIMP) is the most promising technique to generate black and white designs almost free of any gray areas [13].

On the contrary, relatively little effort has been made in simultaneous design for orientation and topology. Pedersen [5, 7] minimized elastic strain energy with two groups of design variables, the material orientation and thickness subjected to a volume constraint. Hansel et al. [14] proposed a heuristic optimization algorithm for minimum weight design of composite laminates based on layer-wise removal of elements with low stress measures. The classical compliance minimization problem was solved for optimal fiber orientations and fiber volume fraction subjected to a fiber cost function constraint by Duvaut et al. [15]. Although their problem formulation is not a topology design formulation, the presented fiber volume fraction distribution resembles the optimal topology. Parnas et al. [16] studied minimum weight design of composite laminates subject to Tsai-Hill failure criterion as stress constraints by sequential quadratic programming. They constructed a bi-cubic Bezier surface for layer thickness representation and cubic Bezier curves for fiber angles and used coordinates of the control points as design variables for reduced number of the design variables.

The above studies lack generality. First, global curve fitting technique often used to represent continuous fiber paths has limited tailorability, restricts fiber paths to a narrow class of pre-defined curves, and cannot be easily generalized for irregular geometries. Second, topology design of laminated composites using evolutionary techniques often lacks a rigorous mathematical basis for optimality. Moreover, variable thickness

laminae are not practical from manufacturing point of view because composite layers are usually produced with fixed thicknesses only. Finally, repeated finite element analyses are usually required which make the design task computationally expensive especially for large scale nonlinear problems.

In the present study, cellular automata (CA) paradigm, a relatively new methodology in structural design, is used to tackle some of the manufacturing issues associated with the optimal fiber orientation design of composite layers as well as high computational costs of the classical methods used in the design. A basic feature of the CA approach is to divide the domain of interest into a large number of cells that typically form a regular grid over the domain. The cells in the domain only interact with their neighboring cells performing local computations. This approach is inherently suitable for parallel implementations because of the local nature of information flow among the neighboring cells and data storage, which does not require keeping information other than local cell level data. Therefore, by employing massively parallel processor machines simulation costs can be considerably reduced.

Recent studies showed the effectiveness of CA based analysis and design in structures such as trusses [17, 18], beams [19], two dimensional isotropic continuum [20], and fiber angle design of composite laminae [21]. In this study, those ideas are extended to design of fiber reinforced composite laminae for in-plane response through combined tailoring of the local fiber orientation angle and topology design. In the following sections, first the optimality criteria for minimum compliance design is given followed by details of the CA implementation. Finally, performance of the proposed algorithm is demonstrated in a series of numerical examples.

2 Minimum Compliance Design

Assume a linearly elastic two-dimensional continuum Ω which has natural boundary condition applied on Γ_1, and essential boundary condition applied on Γ_2, as shown in Figure 1. The point-wise fiber orientation angle relative to a fixed reference X-Y coordinate system at any point in the domain is denoted by $\theta(x, y)$, and a fictitious density measure as proposed in the classical SIMP formulation [13] is represented by $\rho(x, y)$. The design problem is to choose θ and ρ such that the work done by external forces is minimized for applied loads. Denoting the traction vector by $\mathbf{t}$ and displacement vector on Γ_1 by $\mathbf{u}$, the compliance design problem can be written at equilibrium as

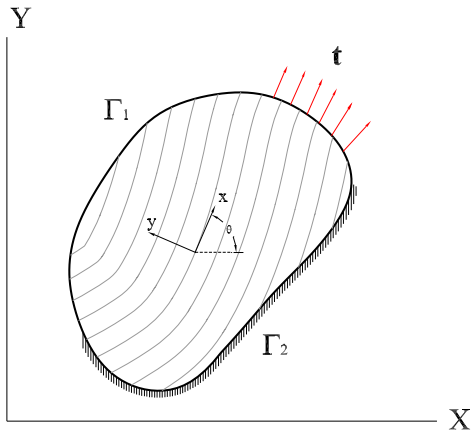

Figure 1: Two dimensional anisotropic domain with curvilinear fibers.

$$\min_{\theta,\rho} \frac{1}{2} \int_{\Gamma_1} \mathbf{t} \cdot \mathbf{u} d\Gamma. \tag{1}$$

In the following subsections, design of fiber angles, and combined topology and fiber angle are explained in detail.

2.1 Fiber Angle Design

Banichuk [11] and Landriani et. al [12] showed that the problem of compliance design will reduce to minimization of the complementary strain energy density $\overline{\Phi}_\sigma$ at any point in the domain of interest,

$$\min_{\theta} \frac{1}{2} \boldsymbol{\sigma} \cdot \overline{\mathsf{Q}}^{-1} \cdot \boldsymbol{\sigma}, \tag{2}$$

where $\boldsymbol{\sigma} = (\sigma_x, \sigma_y, \sigma_{xy})$ is the vector of the 2-D stresses, and $\overline{\mathsf{Q}}$ is the transformed reduced stiffness. Cheng and Pedersen [22] showed that this minimization for fixed stresses is the necessary and sufficient condition for minimum energy, while minimization of the strain energy ($\frac{1}{2}\boldsymbol{\epsilon} \cdot \overline{\mathsf{Q}} \cdot \boldsymbol{\epsilon}$) for fixed strains is only a necessary condition. For the single load case design of a lamina, according to Pedersen [4], the optimal value of the fiber orientation angle that provides the global minimum of this energy density is given by

$$\theta^* = \begin{cases} \varphi; & \text{if } \alpha > 0, \\ \varphi; & \text{if } \alpha < 0 \text{ and } \gamma \leq -1, \\ \varphi + \psi; & \text{if } \alpha < 0 \text{ and } -1 < \gamma < 0, \end{cases} \tag{3}$$

where φ is the principal strain direction

$$\varphi = \frac{1}{2}\arctan\left(\frac{2\epsilon_{xy}}{\epsilon_x - \epsilon_y}\right), \tag{4}$$

and the angle ψ is computed from

$$\psi = \frac{1}{2}\arccos(-\gamma), \tag{5}$$

in which the optimization parameter γ is defined by

$$\gamma = \left(\frac{A_{11} - A_{22}}{A_{11} + A_{22} - 2(A_{12} + 2A_{66})}\right)\left(\frac{1 + \epsilon_{II}/\epsilon_I}{1 - \epsilon_{II}/\epsilon_I}\right), \tag{6}$$

where the A_{ij} denote the elements of the extensional stiffness matrix, and ϵ_I and ϵ_{II} represent principal strains such that $|\epsilon_I| > |\epsilon_{II}|$. The engineering properties in the material coordinate system are denoted by E_1, E_2, G_{12}, and ν_{12}. The non-dimensional material constant α [3] is defined as

$$\alpha = 1 + (E_2/E_1)(1 - 2\nu_{12}) - 4(G_{12}/E_1)(1 - \nu_{12}^2 E_2/E_1). \tag{7}$$

In the case of design for multiple loads, a weighted average compliance minimization technique is used. In this method, the problem is posed as minimization of the weighted sum of individual compliances

$$\min_{\theta} \sum_{i=1}^{L} w_i W_c^{(i)}, \tag{8}$$

where $W_c^{(i)}$ is the compliance of the i^{th} load case, L is the number of load cases, and the w_i are the positive weighting factors such that $\sum_{i=1}^{L} w_i = 1$. This problem also reduces to minimization of the weighted average of the complimentary strain energy densities at any point in the domain:

$$\Phi^* = \min_{\theta} \sum_{i=1}^{L} w_i \overline{\Phi}_{\sigma}^{(i)}. \tag{9}$$

Bendsøe and Sigmund [13] showed that the above minimization problem translates to finding the roots of a fourth order polynomial in terms of $\sin 2\psi$. However, in the present study, a numerical one-dimensional optimizer is used.

2.2 Combined Fiber Angle and SIMP Topology Design

In the case of combined fiber angle and topology design, in addition to the fiber angle, a density measure $0 \leq \rho(x, y) \leq 1$ is also designed at any point. As shown by Setoodeh et al. [23], the optimality criterion for minimum compliance design splits into two levels. In the first level, fiber angle at any point is designed for minimum complimentary strain energy density defined in Equation 9. In the second level, the topology design, the following density update is used

$$\rho = \begin{cases} \hat{\rho} & \varepsilon < \hat{\rho} < 1 \\ \varepsilon & \hat{\rho} < \varepsilon \\ 1 & \hat{\rho} > 1 \end{cases} \tag{10}$$

where ε is a small number used to avoid numerical ill conditioning and,

$$\hat{\rho} = \left(\frac{\Phi^*}{\overline{\mu}} \right)^{\frac{1}{p+1}} . \tag{11}$$

The optimal complimentary strain energy Φ^* in this equation is obtained in the previous level from Equation 9, $\overline{\mu}$ is a constant which can be loosely interpreted as an average strain energy density in the structure, and p is the density penalization parameter.

3 Structural Design Using Cellular Automata

The cellular automata paradigm is based on discretization of the physical domain of a problem into a lattice of regular cells that compute and communicate with their neighboring cells only [24]. Essentially, a cellular automaton consists of a set of identical components governed by simple rules acting together to predict complicated behavior of a system. These small components (cells) interact with a group of adjacent cells known as a neighborhood. This neighborhood can be any group of cells, however, in this study the classical *Moore* neighborhoods is used. The Moore neighborhood shown in Figure 2-(a) is a 3×3 square grid of cells described by the center cell and cells located at directions SW, S, SE, W, E, NW, N, and NE.

Point-wise quantities associated with each cell constitute *cell state* information and are updated concurrently in discrete time steps using prespecified rules. The state of a cell at iteration t is denoted by $\phi^{(t)}$ and

may consist of numeric, logical, and character entries. For combined topology and fiber angle design in two dimensions, we define the state of the i-th cell as:

$$\phi_i = \{(u_i, v_i), (f_{x_i}, f_{y_i}), (\rho_i, \theta_i), \overline{\mathsf{Q}}\} \tag{12}$$

where u_i and v_i are the cell displacements in x and y directions respectively, f_{x_i} and f_{y_i} are the external forces acting on the i-th cell in the corresponding directions. Density measure and fiber angle of the cell are denoted by ρ_i and θ_i and $\overline{\mathsf{Q}}$ is the reduced transformed stiffness which due to symmetry only the upper half diagonal of the matrix is stored (six elements).

In a serial implementation for a regular lattice, cells are updated starting from the lower left corner to upper right corner in a row-wise fashion. During this update process, each cell uses only its own state and the latest state information of the neighboring cells. For instance, for a Moore neighborhood, a serial Gauss-Seidel update process can be written as follows:

$$\phi_C^{(t+1)} = \Re(\phi_{SW}^{(t+1)}, \phi_S^{(t+1)}, \phi_{SE}^{(t+1)}, \phi_W^{(t+1)}, \phi_C^{(t)}, \phi_E^{(t)}, \phi_{NW}^{(t)}, \phi_N^{(t)}, \phi_{NE}^{(t)}), \tag{13}$$

where $\Re$ is the update rule. This iterative update process is then terminated when changes in the cell state for all cells in the entire lattice are less than a tolorance. Such a serial implementation of a CA model for analysis is completely equivalent to the classical Gauss-Seidel matrix iteration, with the update rules suitably interpreted as pointwise equilibrium conditions defining a global system of equations ($\mathbf{KX} = \mathbf{F}$).

The update rule for the present problem has two parts: *analysis update* and *design update* . The analysis rule updates the displacements of the site cell given the neighboring cell displacements. This rule is governed by the equilibrium of the local neighborhood for the case of in-plane deformations. As shown in the previous section, the local design update rule splits into two levels. In the first level, the fiber angle is updated such that the complimentary strain energy is minimized. Using this new fiber angle, the second level updates density of the cell. In the following sections these update rules are described in detail.

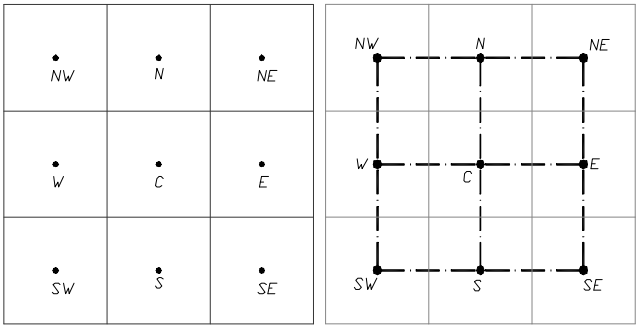

(a) Moore neighborhood. (b) Moore bilinear model.

Figure 2: CA Moore neighborhood.

3.1 Analysis Update Rule

Four bilinear quadrilateral elements are used to prepare the local analysis update model as shown in Figure 2-(b). Each element is assumed to have constant thickness and material properties given by:

$$\frac{1}{\overline{\rho}^p} = \frac{1}{4}\sum_{i=1}^{4}\frac{1}{\rho_i^p} \tag{14}$$

$$\overline{\mathsf{Q}} = \frac{1}{4}\sum_{i=1}^{4}\mathsf{Q}_i \tag{15}$$

where ρ_i's and Q_i's are respectively the density measures and reduced in-plane stiffness at the four nodes of the element. The density interpolation scheme is chosen such that any node with a density measure below the threshold value ε would turn-off all four elements in which the node participates.

The equilibrium equation of the local neighborhood can be written in the following matrix form:

$$\begin{bmatrix} \mathbf{K}_{nn} & \mathbf{K}_{nc} \\ \mathbf{K}_{cn} & \mathbf{K}_{cc} \end{bmatrix} \begin{Bmatrix} \mathbf{u}_n \\ \mathbf{u}_c \end{Bmatrix} = \begin{Bmatrix} \mathbf{f}_n \\ \mathbf{f}_c \end{Bmatrix}, \tag{16}$$

where $\mathbf{u}_c = \{u_i, v_i\}$ and $\mathbf{f}_c = \{f_{x_i}, f_{y_i}\}$ are the site cell displacements and external forces respectively. Displacements and external forces of the neighboring cells are denoted by $\mathbf{u}_n$ and $\mathbf{f}_n$ and $\mathbf{K}$'s are the

stiffness matrices of the local model (see the appendix for element stiffness matrix expressed in terms of the laminate extensional stiffness). The second row of this equation can be written as

$$\mathbf{K}_{cc}\mathbf{u}_c - \mathbf{f}_c = -\mathbf{K}_{cn}\mathbf{u}_n \tag{17}$$

knowing displacement of the neighboring cells and stiffness matrices, i.e., $\mathbf{u}_n$ and $\mathbf{K}$'s, and given any pair of $(u_i, v_i, f_{x_i}, f_{y_i})$, Equation (17) is solved numerically for the remaining pair. In a CA based analysis, this update rule is applied to all cells in the lattice iteratively in a Gauss-Siedel fashion until displacements of all cells are converged in the following relative sense:

$$\frac{\|{\mathbf{u}_c}^{new} - {\mathbf{u}_c}^{old}\|}{\|{\mathbf{u}_c}^{old}\|} \leq \epsilon, \tag{18}$$

where $\mathbf{u}_c^{old}$ and $\mathbf{u}_c^{new}$ are the cell displacements before and after update respectively.

In a CA combined analysis and design, the design update rule is activated before full convergence in the displacement filed is achieved. This activation occurs whenever the displacements are converged in a looser sense as compared to the main termination criterion of Equation (18). For instance, in this study the displacement convergence tolerance is set to be $\epsilon = 10^{-6}$ and design is turned on at $\epsilon = 10^{-4}$. Cell stresses/strains are computed by averaging their corresponding values at the closest Barlow [25] points to the center node over active quadrants.

3.2 Design Update Rule

Once cell displacements were updated using the analysis update rule, Equations (9) and (10) are used to update fiber angle and density respectively. Cell stresses and complimentary strain energy density are computed by averaging their corresponding values at the closest Barlow points of the active quadrants to the center cell. For instance, the complimentary strain energy density is computed from

$$\Phi^* = \frac{1}{N_{cell}} \sum_{i=1}^{N_{cell}} \frac{1}{2} \bar{\rho}_i^{2p} {\boldsymbol{\sigma}_i}^T . \overline{\mathbf{Q}}_i^{-1} . \boldsymbol{\sigma}_i \tag{19}$$

in which N_{cell} is the number of active quadrants.

3.3 Heuristic Pattern Matching

For complex geometries in which the stress state changes rapidly in some regions of the layer, the optimal fiber orientation angle can also change rapidly. For example, in the case of layers with a hole or cutout stress concentration near the hole boundary may cause the fiber orientation to change rapidly. It is also observed that in some cases, at locations where the stresses are very low, the principal stress direction varies erratically due to roundoff error. In either case, fabricating such laminates with rapidly varying fiber orientation angles may be difficult, if not impossible, if curvilinear fiber orientation designs are sought.

To resolve this problem and achieve local fiber orientation continuity, a cell level heuristic manufacturing improvement update scheme is applied along with the strain energy minimization design scheme. In this heuristic approach, in some cases the optimal cell fiber angle, computed from the optimality criterion, is replaced with a new angle that matches the orientation of the neighboring cells. This is accomplished by using a *pattern matching* technique to establish a neighborhood pattern if one exists. To form the neighborhood pattern, the continuous fiber angles for the Moore neighborhood are first rounded to the nearest discrete orientations according to the rule

$$\theta^* = \begin{cases} 90°; & \theta \geq 67.5° \text{ or } \theta < -67.5°, \\ -45°; & -67.5° \leq \theta < -22.5°, \\ 0°; & -22.5° \leq \theta < 22.5°, \\ 45°; & 22.5° \leq \theta < 67.5°. \end{cases} \tag{20}$$

Note that the rounded neighborhood angles are only used for the pattern matching process, and the angles of the neighboring cells are left unchanged. Once the neighborhood fiber angles are rounded, if any five *adjacent neighborhood cells* have the same discrete fiber orientation, then a pattern is said to be formed. For the Moore neighborhood with eight cells, there are eight possible pattern shapes. Four of the patterns are "C" shaped (e.g., N-NW-W-SW-S or W-NW-N-NE-E) and four are "L" shaped (e.g., NW-W-SW-S-SE or NE-E-SE-S-SW), see Figure 2 (a). For a neighborhood with a formed pattern, the optimal angle from Equation (3) is also rounded using Equation (20), then it is checked against the matched direction. If they disagree, the site cell angle is replaced with the average value of the continuous angles of the cells that formed the pattern. If they agree, or if the neighborhood does not form a pattern, then the optimal angle is used to update the cell angle.

In order to enhance the convergence of the algorithm, the pattern matching scheme is activated when the displacement field is loosely converged compared to the CA convergence criterion. This ensures that the information has reached every part of the domain and all possible patterns have been formed.

4 Results

A Fortran90 code was implemented based on the methodology described in this paper which runs on a serial machine. The same frame work has been extended to message-passing multiprocessor [26], where details of parallel implementation is provided along with performance studies.

To demonstrate performance of the proposed update rules, first fiber angle design of composite laminae is considered. Then combined fiber angle and topology design for both single and multiple load cases is presented. In all the simulations, the penalization parameter p is set to 3 and the reported complinaces are normalized with respect to a 0° fiber design. The following material properties are used for all examples unless specified otherwise:

$$\frac{E_1}{E_2} = 14.6, \qquad \frac{G_{12}}{E_2} = 0.68, \qquad \nu_{12} = 0.318. \tag{21}$$

4.1 Short Cantilever

Fiber angle design of a short cantilever with aspect ratio of three and a uniformly distributed load of 1.0 kN/m (cf. Figure 3-(a)) is considered as suggested by Pedersen [7]. The material properties used in the simulations are

$$\frac{E_1}{E_2} = 8.0, \qquad \frac{G_{12}}{E_2} = 0.35, \qquad \nu_{12} = 0.3. \tag{22}$$

Optimal designs for different CA lattice densities are depicted in Figure 3-(b) through Figure 3-(d), and Table 1 lists the corresponding compliances. Compliance for 46×16, 91×31, and 301×101 lattices are improved by a factor of $2.6 = 746.2/290.5$, $2.7 = 813.3/298.4$, and $3.0 = 929.0/310.6$, respectively. These results show that the optimal design is nearly independent of the lattice density and also the compliance improvements remain rather unchanged.

Table 1: Compliance of the short cantilever.

	Compliance $(N \cdot m)$	
CA Lattice	0° **Fibers**	**Optimal Design**
46×16	746.2	290.5
91×31	813.3	298.4
301×101	929.0	310.6

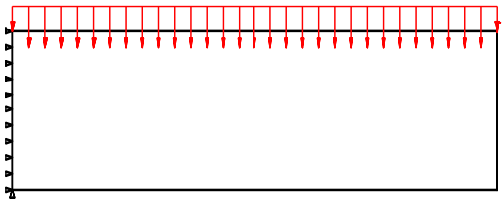

(a) Short cantilever with uniformly distributed loading.

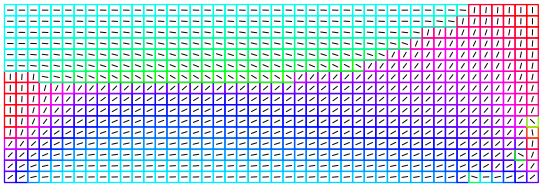

(b) 46×16 CA lattice.

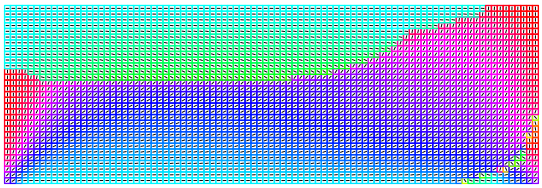

(c) 91×31 CA lattice.

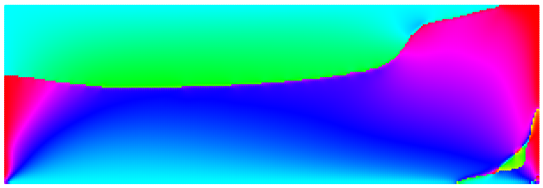

(d) 301×101 CA lattice.

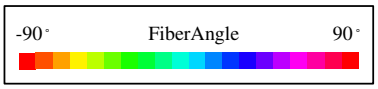

Figure 3: Cantilever design with different CA cell densities.

4.2 Cutout problem

The CA design methodology is demonstrated for a square plate with a center cutout. The ratio of the width to the hole diameter for this plate is 3, and it is loaded with a uniform shear load. It is assumed that a quarter plate, as shown in Figures 4-(a), can be used to model the problem. A 61×61 CA lattice is used

for the analysis and the design of this quarter model.

Figure 4-(b) shows the CA fiber angle distribution results for the quarter model in shear loading. Although compliance is improved by 65% without pattern matching, this design has fiber discontinuities that are probably not practical. Figure 4-(c) shows the results with the proposed heuristic pattern matching gaining 55% compliance improvement.

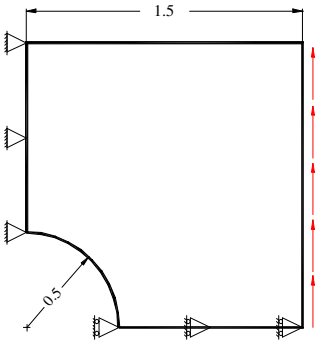

(a) Geometry and loading.

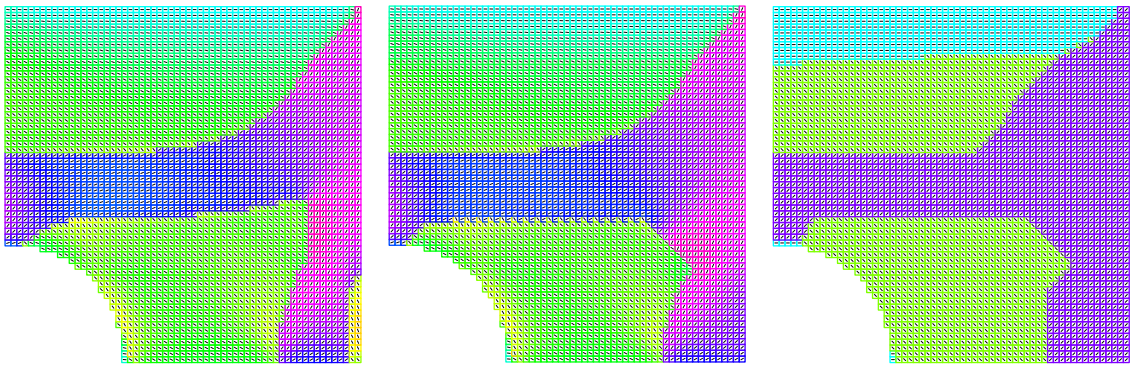

(b) Optimality criteria. (c) Pattern matching. (d) Discrete pattern matching.

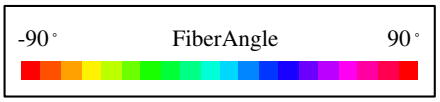

Figure 4: Cutout example in shear (61×61 CA cells).

With a rule based design update scheme for the cells, it is also possible to implement other rules beyond the one implemented to establish neighborhood fiber orientation continuity. For example, it is possible that

the values of the design variables be chosen out of a set of discrete values rather than using their continuous or pattern matching results. In the case of composite laminate design, it is customary to use discrete fiber orientation angles such as $0°, -45°, 45°, 90°$. The resulting fiber orientation pattern by implementing a discrete fiber orientation rule with fiber angles rounded to $0°, -45°, 45°, 90°$ angles along with pattern matching are shown in Figure 4-(d) for the case of shear loading. For the numerical implementation, the cell fiber angles are kept fixed and CA analysis is performed until full convergence of the displacement fields. Once the discrete angle rule is activated, the iterations are continued until the design and analysis are again converged. The resulting design shown in the figure has a normalized compliance of 0.46 which is almost the same as the result obtained for the design with pattern matching alone. As this figure shows, the presented heuristic pattern matching technique generates patches of similar discrete fiber orientations and resolves some of the manufacturing issues further. Based on the authors' experience, it may be possible to manufacture such fiber reinforced layers using advanced tow-placement machines that have the capability to cut and restart individual tows during fabrication. Table 2 tabulates the normalized compliances for the shear test problem.

Table 2: Normalized compliance of the cutout example (61×61 CA cells).

Design	**Normalized Compliance**
$0°$ Fibers	1.0
Optimality Criterion	0.35
Pattern Matching	0.45
Discrete Pattern Matching	0.46

4.3 Symmetric Cantilever

We next consider the case of combined fiber angle and topology design, where cell density is used to eliminate material from cells with lower strain energy density levels. The symmetric cantilever plate in Figure 5-(a) with aspect ratio of 4 is modeled with a regular lattice of 325×82 CA cells. Figures 5-(b) through 5-(e) show the optimal designs for different volume fractions for which the normalized compliances are tabulated in Table 3. These figures show that with the present choice of density interpolation scheme checkerboards are readily suppressed.

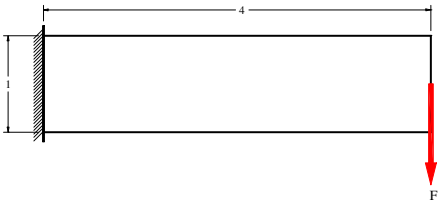

(a) Geometry and loading.

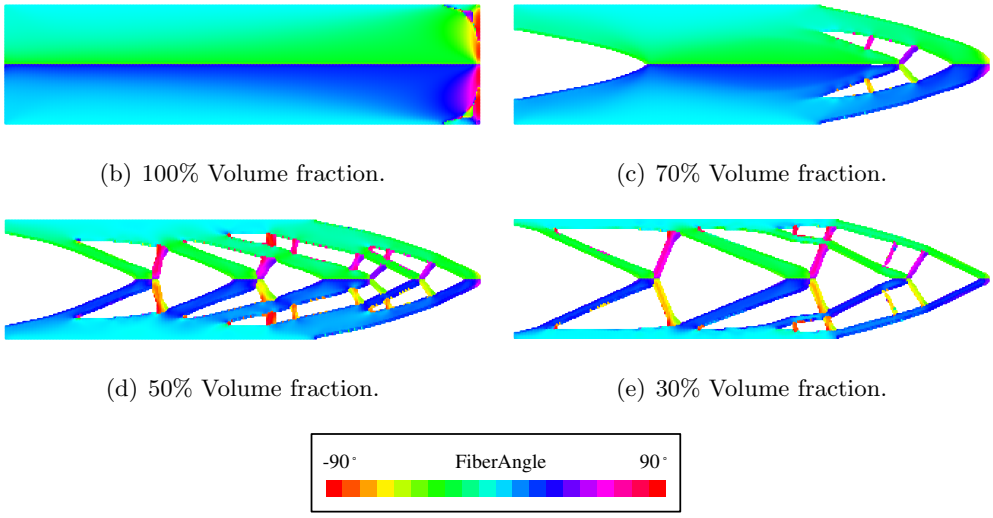

(b) 100% Volume fraction.

(c) 70% Volume fraction.

(d) 50% Volume fraction.

(e) 30% Volume fraction.

Figure 5: Optimal topology of the symmetric cantilever (325×82 cells).

Table 3: Normalized compliance of the symmetric cantilever problem for different volume fractions (325×82 CA cells).

Volume Fraction(η)	$\bar{C}$
1.00	0.74
0.70	0.86
0.50	1.19
0.30	2.26

4.4 Asymmetric Cantilever Multiple Load Case

The asymmetric cantilever of Figure 6-a is considered here to demonstrate the multiple load case design. The first load case is a downward load as denoted by F_1 in the figure, and the upward load F_2 with the same

magnitude is the second load case. Optimal design for several volume fractions are depicted in Figure 6 and numerical values for the corresponding normalized compliance are tabulated in Table 4.

Table 4: Normalized compliance of the asymmetric cantilever for multiple load case design. (203×102 CA cells)

Volume Fraction(η)	**Normalized Compliance**($\bar{C}$)
1.00	0.32
0.90	0.33
0.70	0.40
0.50	0.57

4.5 Extended Optimality

The optimum topology can be obtained for different volume fractions. As the volume fraction decreases, the compliance will increase. Consider a non-dimensional compliance defined by:

$$\overline{C} = \frac{C_i \eta_i}{C_0} \tag{23}$$

where C_i is the corresponding compliance for a volume fraction of η_i and C_0 is the compliance for $\eta = 1.0$. Figure 7 shows variations of this non-dimensional compliance for different cantilever problems as a function of volume fraction. In the present formulation where compliance is minimized with a given volume fraction for prescribed loads, it makes practical sense to minimize the non-dimensional compliance as defined in Equation (23). Following Rozvany et al. [27], this new design is optimal in an *extended optimality* sense. This can also be interpreted as maximization of the performance index of the design as described in [28]. Figure 7 predicts that the optimal designs in the sense of extended optimality for the symmetric, asymmetric single load case, and asymmetric multiple load case correspond approximately to $\eta = 0.60$, $\eta = 0.40$, and $\eta = 0.50$ respectively.

5 Conclusions

This study has demonstrated a cellular automata based methodology for in-plane analysis and design of two-dimensional orthotropic media. The analysis is based on the equilibrium of local cells and the design process uses the optimality criterion for compliance minimization. Numerical studies on different problems showed a good rate of convergence, robustness, and mesh independency of the proposed algorithm. Application of the presented heuristic pattern matching technique generates patches of similar fiber orientations and resolves some of the manufacturing issues. A multiple load case design was also investigated using the weighted average compliance minimization technique. It was shown that substantial gains in compliance can be achieved through placement of fibers in their optimal spatial configuration. The density interpolation scheme readily suppresses checkerboards and the algorithm is free of numerical instabilities.

6 Appendix

The stiffness matrix in two-dimension for the bilinear element is expressed in the following form;

$$\mathbf{K}^e = \begin{bmatrix} \mathbf{K}^{11} & \mathbf{K}^{12} \\ symm. & \mathbf{K}^{22} \end{bmatrix} \tag{24}$$

These stiffness sub-matrices are given in terms of the laminate extensional stiffness $\mathbf{A}$ as follows [29]:

$$\mathbf{K}^{11} = A_{11}\mathbf{S}^{xx} + A_{13}(\mathbf{S}^{xy} + \mathbf{S}^{yx}) + A_{33}\mathbf{S}^{yy},$$

$$\mathbf{K}^{12} = A_{12}\mathbf{S}^{xy} + A_{13}\mathbf{S}^{xx} + A_{23}\mathbf{S}^{yy} + A_{33}\mathbf{S}^{yx},$$

$$\mathbf{K}^{22} = A_{33}\mathbf{S}^{xx} + A_{23}(\mathbf{S}^{xy} + \mathbf{S}^{yx}) + A_{22}\mathbf{S}^{yy}.$$

where the elements of the $\mathbf{S}$ matrix are defined as:

$$S_{ij}^{\xi\eta} = \int_{\Omega_e} \frac{\partial\psi_i}{\partial\xi}\frac{\partial\psi_j}{\partial\eta}dxdy \tag{25}$$

in which ψ_i $(i = 1, ..., 4)$ is the bilinear element interpolation function. In the case of square bilinear elements, $\mathbf{S}^{xx}$, $\mathbf{S}^{xy}$, and $\mathbf{S}^{yy}$ are computed exactly as the followings;

$$\mathbf{S}^{xx} = \begin{bmatrix} \frac{1}{3} & -\frac{1}{3} & -\frac{1}{6} & \frac{1}{6} \\ -\frac{1}{3} & \frac{1}{3} & \frac{1}{6} & -\frac{1}{6} \\ -\frac{1}{6} & \frac{1}{6} & \frac{1}{3} & -\frac{1}{3} \\ \frac{1}{6} & -\frac{1}{6} & -\frac{1}{3} & \frac{1}{3} \end{bmatrix}, \tag{26}$$

$$\mathbf{S}^{yy} = \begin{bmatrix} \frac{1}{3} & \frac{1}{6} & -\frac{1}{6} & -\frac{1}{3} \\ \frac{1}{6} & \frac{1}{3} & -\frac{1}{3} & -\frac{1}{6} \\ -\frac{1}{6} & -\frac{1}{3} & \frac{1}{3} & \frac{1}{6} \\ -\frac{1}{3} & -\frac{1}{6} & \frac{1}{6} & \frac{1}{3} \end{bmatrix}, \tag{27}$$

$$\mathbf{S}^{xy} = \begin{bmatrix} \frac{1}{4} & \frac{1}{4} & -\frac{1}{4} & -\frac{1}{4} \\ -\frac{1}{4} & -\frac{1}{4} & \frac{1}{4} & \frac{1}{4} \\ -\frac{1}{4} & -\frac{1}{4} & \frac{1}{4} & \frac{1}{4} \\ \frac{1}{4} & \frac{1}{4} & -\frac{1}{4} & -\frac{1}{4} \end{bmatrix}, \tag{28}$$

$$\mathbf{S}_{yx} = \mathbf{S}_{xy}^T. \tag{29}$$

References

[1] Evans, D. O., Vaniglia, M. M., and Hopkins, P. C., "Fiber Placement Process Study," *34th International SAMPE Symposium and Exhibition*, May 1989, pp. 1822–1833.

[2] Brandmaier, H. E., "Optimum Filament Orientation Criteria," *J. Composite Materials*, Vol. 4, July 1970, pp. 422–425.

[3] Pedersen, P., "On Optimal Orientation of Orthotropic Materials," *Structural Optimization*, , No. 1, 1989, pp. 101–106.

[4] Pedersen, P., "Bounds on Elastic Energy in Solids of Orthotropic Materials," *Structural Optimization*, Vol. 2, 1990, pp. 55–63.

[5] Pedersen, P., "On Thickness and Orientational Design with Orthotropic Materials," *Structural Optimization*, , No. 3, 1991, pp. 69–78.

[6] Pedersen, P., "Optimal Orientation of Anisotropic Materials, Optimal distribution of anisotropic materials, optimal shape design with anisotropic materials, optimal design for a class of non-linear elasticity," *Optimization of Large Structural Systems*, edited by G. I. N. Roozvany, Vol. II, 1993, pp. 649–681.

[7] Pedersen, P., "Examples of Density, Orientation, and Shape-Optimal 2D-Design for Stiffness and/or Strength with Orthotropic Materials," *Structural Optimization*, Vol. 26, No. 1-2, 2003, pp. 37–49.

[8] Hyer, M. W. and Charette, R. F., "Use of Curvilinear Fiber Format in Composite Structure Design," *AIAA*, Vol. 29, No. 6, 1991, pp. 1011–1015.

[9] Katz, Y., Haftka, R. T., and Altus, E., "Optimization of Fiber Directions for Increasing the Failure Load of a Plate with a Hole," *4th ASC Technical Conference*, Vol. 4, Blacksburg, VA, October 1989, pp. 62–71.

[10] Nagendra, S., Kodiyalam, S., and Davis, J. E., "Optimization of Tow Fiber Paths for Composite Design," *Proceedings of the AIAA/ASME/ASCE/AHS/ASC* 36^{th} *SDM Conference*, New Orleans, LA, April 10-13 1995, pp. 1031–1041.

[11] Banichuk, N. V., "Optimization of Anisotropic Properties of Deformable Media in Plane Problems of Elasticity," *Mechanics of Solids*, Vol. 14, No. 1, 1979, pp. 63–68.

[12] Landriani, G. S. and Rovati, M., "Optimal Design for Two-Dimensional Structures Made of Composite Materials," *Transactions of the ASME*, Vol. 113, 1991, pp. 88–92.

[13] Bendsøe, M. P. and Sigmund, O., *Topology Optimization, Theory, Methods and Applications*, Springer-Verlag, Berlin Heidelberg New York, 2003.

[14] Hansel, W. and Becker, W., "Layerwise adaptive topology optimization of laminate structures," *Engineering Computations*, Vol. 16, No. 7, 1999, pp. 841–851.

[15] Duvaut, G., Terrel, G., Léné, F., and Verijenko, V. E., "Optimization of Fiber Reinforced Composites," *Composite Structures*, Vol. 48, 2000, pp. 83–89.

[16] Parnas, L., Oral, S., and Ceyhan, U., "Optimum design of composite structures with curved fiber courses," *Composite Science and Technology*, Vol. 63, 2003, pp. 1071–1082.

[17] Gürdal, Z. and Tatting, B., "Cellular Automata for Design of Truss Structures with Linear and Nonlinear Response," *Proceedings of the 41st AIAA/ASME/ASCE/AHS Structures, Structural Mechanics and Materials Conference*, AIAA Paper, Atlanta, GA, 2000, pp. 2000–1580.

[18] Tatting, B. and Gürdal, Z., "Cellular Automata for Design of Two-Dimensional Continuum Structures," *Proceedings of the 8th AIAA/USAF/NASA/ISSMO Symposium on Multidisciplinary Analysis and Optimization*, AIAA Paper, Long Beach, CA, 2000, pp. 2000–4832.

[19] Abdalla, M. and Gürdal, Z., "Structural Design Using Cellular Automata for Eigenvalue Problems," *6th US National Congress on Computational Mechanics*, Dearborn, MI, 2001.

[20] Abdalla, M. and Gürdal, Z., "Structural Design Using Optimality Based Cellular Automata," *Proceedings of the 43rd AIAA/ASME/ASCE/AHS Structures, Structural Mechanics and Materials Conference*, AIAA, Denver, CO, 2002, pp. 2002–1676.

[21] Setoodeh, S. and Gürdal, Z., "Design of Composite Layers with Curvilinear Fiber Paths Using Cellular Automata," *Proceedings of the 44th AIAA/ASME/ASCE/AHS Structures, Structural Dynamics, and Materials Conference*, Norfolk, Virginia, 7-10 April 2003.

[22] Cheng, G. and Pedersen, P., "On Sufficiency Conditions for Optimal Design Based on Extremum Principles of Mechanics," *J. Mech. Phys. Solids*, Vol. 45, No. 1, 1997, pp. 135–150.

[23] Setoodeh, S., Gürdal, Z., and Abdalla, M. M., "Simultaneous Topology and Curvilinear Fiber Path Design of Composite Layers Using Cellular Automata," *Proceedings of the 45th AIAA/ASME/ASCE/AHS/ASC SDM Conference*, Palm Spring, California, April 18-22 2004, pp. 1–2.

[24] Preston, K. and Duff, M. J. B., *Modern Cellular Automata, Theory and Applications*, Plenum Press, New York, 1984.

.

[25] Barlow, J., "Optimal Stress Locations in Finite Element Models," *Int. J. Numer. Methods Eng.*, Vol. 10, 1976, pp. 243–251.

[26] Setoodeh, S., Adams, D. B., Gürdal, Z., and Watson, L. T., "Pipeline Implementation of Cellular Automata for Structural Design on Message-Passing Multiprocessors," Mathematical and Computer Modeling, to appear.

[27] Rozvany, G., Querin, O., and Pomezanski, V., "Extended optimality in topology design," *Struct Multidisc Optim*, Vol. 24, 2002, pp. 257–261.

[28] Liang, Q. Q. and Steven, G. P., "A performance-based optimization method for topology design of continuum structures with mean compliance constraints," *Comput. Methods Appl. Mech. Engrg.*, Vol. 191, 2002, pp. 1471–1489.

[29] Reddy, J. N., *Mechanics of Laminate Composite Plates, Theory and Analysis*, CRC Press, 1997.

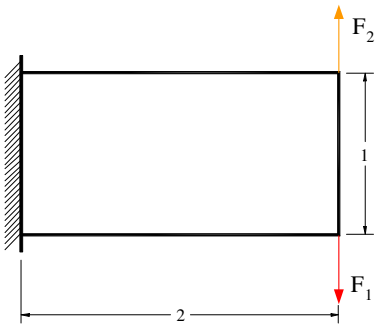

(a) Geometry and loading.

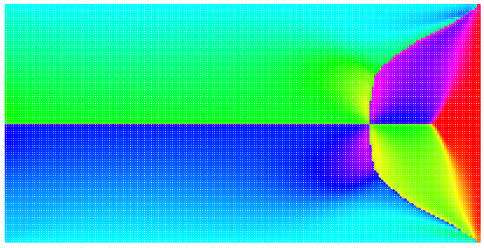

(b) 100% Volume fraction.

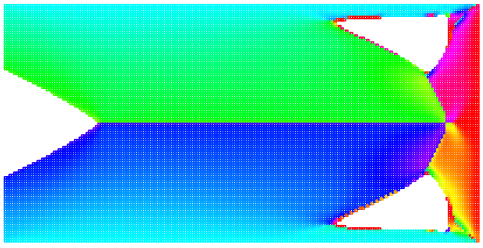

(c) 90% Volume fraction.

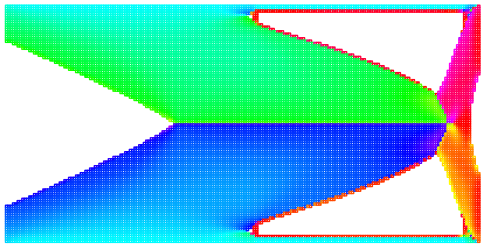

(d) 70% Volume fraction.

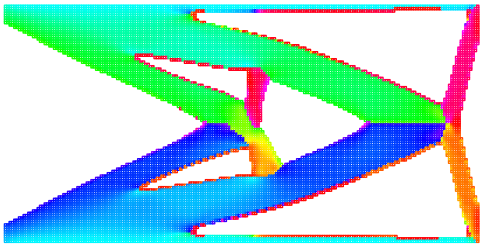

(e) 50% Volume fraction.

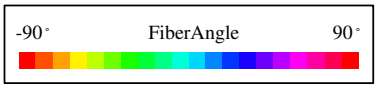

Figure 6: Optimal topology for multiple load case design of the asymmetric cantilever (203×102 cells).

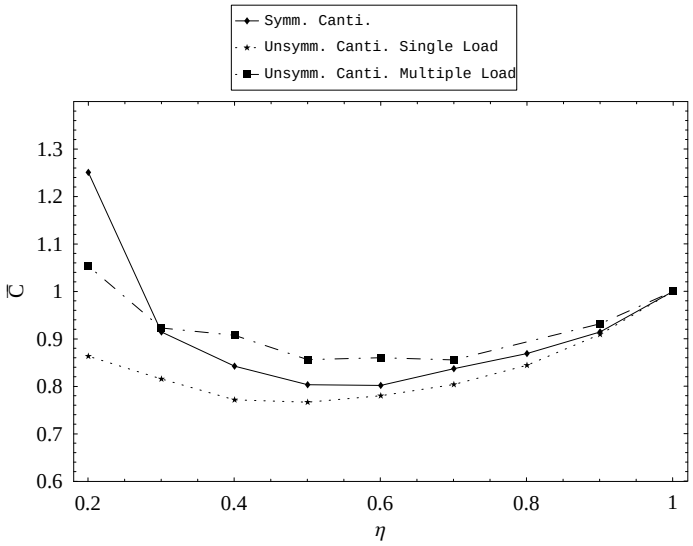

Figure 7: Nondimensional compliance as a function of volume fraction.